# Evidence for a Basalt-Free Surface on Mercury and Implications for Internal Heat

Raymond Jeanloz,* David L. Mitchell, Ann L. Sprague, Imke de Pater

**Microwave and mid-infrared observations reveal that Mercury's surface contains less FeO + $TiO_2$ and at least as much feldspar as the lunar highlands. The results are compatible with the high albedo (brightness) of Mercury's surface at visible wavelengths in suggesting a rock and soil composition that is devoid of basalt, the primary differentiate of terrestrial mantles. The occurrence of a basalt-free, highly differentiated crust is in accord with recent models of the planet's thermal evolution and suggests that Mercury has retained a hot interior as a result of a combination of inefficient mantle convection and minimal volcanic heat loss.**

Twenty years after the first and only flybys imaging its surface, Mercury remains one of the most enigmatic planets in the solar system (*1–3*). The presence of a weak magnetic field (surface intensity ~0.7% of that of Earth) most likely implies that at least part of Mercury's large metallic core is molten (*4–6*). Yet the small planetary radius suggests that Mercury's interior should have cooled relatively quickly by means of processes of mantle convection and volcanic eruption that are thought to control the thermal evolution of the terrestrial planets (*5–7*). Indeed, one can infer from recent model calculations that "heat piping," the loss of heat from the deep interior through volcanism, should have frozen out Mercury's core long ago (*7*).

Basaltic volcanism is particularly significant in this context because basalt represents the liquid formed upon the partial melting of a terrestrial planetary mantle (*5, 8, 9*). Thus, extraction of basalt is the primary means by which the rocky (silicate) fractions of planets undergo geochemical differentiation and concomitant volcanic heat loss from the interior (*5*). Dynamical considerations indicate that as much as 50% of Mercury's crust-mantle system can be tapped by basaltic magmas (*10*). That is, a large fraction of the interior has been subject to volcanic cooling: far more than the geologically active Earth and Venus (<10%) and comparable in magnitude to the moon (~65%) and Mars (~25%), which have now evolved toward geological senescence.

The amount, and even the presence, of volcanic rocks on Mercury's surface is controversial, according to photogeological studies (*1–3, 5*). Here we focus on the more specific question of whether basalts are present in abundance on the surface of Mercury. In accordance with current models of the planet's formation and earliest evolution, our presumption is that Mercury's mantle is essentially chondritic or peridotic in bulk composition, with the unusually large core and high Fe/Si ratio of the planet due to a late-stage giant impact (*3, 11–14*).

We begin by modeling microwave images of Mercury's thermal emissions at frequencies of 4.8 to 100 GHz (wavelengths 6.2 to 0.3 cm) (*15*). The overall appearance of Mercury at these wavelengths (Fig. 1A) is influenced by the planet's unique diurnal heating pattern, resulting from a 3:2 spin-orbit resonance in combination with a large orbital eccentricity ($e = 0.2$) (*15, 16*). The effects of this diurnal heating pattern are wavelength-dependent and have been modeled to produce a residual image that is obtained by subtracting a best fit model from the thermal image (Fig. 1B). The microwave opacity is adjusted in the model so as to reproduce diurnal brightness variations across the disk (*15*).

The result is that Mercury's regolith is found to be remarkably transparent to microwaves: at least two times as transparent as the lunar maria and at least 1.4 times as transparent as the lunar highlands throughout the frequency range examined (*15*). The dielectric loss tangents of Mercury's surface are lower, at comparable frequencies, than those of samples from either Earth or the moon (Fig. 2). Also, extrapolation of temperature- and frequency-dependent laboratory measurements shows that no more than ~1 to 10% $CaTiO_3$ perovskite can be present on the surface of Mercury (*17*). As $CaTiO_3$ perovskite is a significant mineral among high-temperature condensates of the solar nebula (*3, 18*), our finding that it cannot be very abundant on the surface and the observation that an alkali-rich atmosphere is present around the planet (*19*) both argue against a particularly refractory composition for Mercury's crust (*13*).

To interpret the dielectric loss tangent in terms of whole-rock composition, all values are referred to a common frequency of 450 MHz, for which numerous laboratory measurements exist. This involves extrapolating the Mercury data to lower frequencies than observed, which we do by averaging the frequency dependencies of the microwave observations and of the laboratory data as indicated in Fig. 2. A total FeO + $TiO_2$ content of 1.2% (by weight) is thus inferred for Mercury's surface on the basis of the empirical correlation of Heiken *et al.* (*20*) between composition and dielectric loss tangent (Fig. 3). All uncertainties combined are estimated to bound the surface

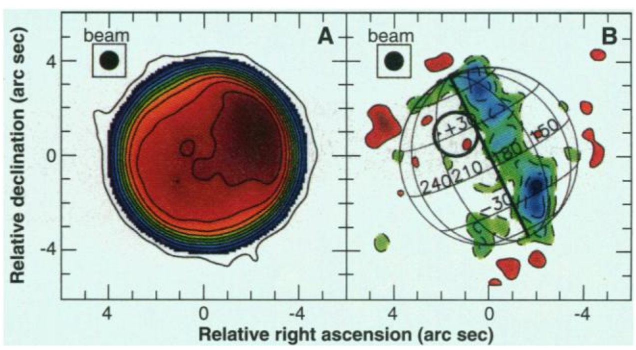


**Fig. 1.** (**A**) Image of Mercury's thermal emission at 23 GHz (1.3-cm wavelength), with intensity expressed in units of brightness temperature (crudely, an average of the physical temperature within the upper ~35 cm of the regolith), color-coded from blue (cold) to red (hot). Contours are at 10% steps from the maximum of 393 K, except for the lowest contour which is at the 2% (8 K) level. The resolution (inset) is 520 km on Mercury's surface, and the image was obtained in August 1990, when the planet was at the greatest eastern elongation (*15*). (**B**) Residual image showing deviations from the best fit model to the thermal image; see (*15*) for further details. Blue regions are cooler than the model and red regions are warmer. The 5-K contour interval (dashed = negative) is roughly three times the root mean square noise. The planet's orientation is indicated by lines of constant longitude and latitude at 30° intervals; the bold line is the morning terminator, and the sunlit hemisphere is on the right. The bold circle outlines the main rim of the Caloris Basin. Negative residuals (thermal depressions) along the sunlit side of the terminator result from shadows cast by hills and crater walls that were not included in the model.

R. Jeanloz, Department of Geology and Geophysics, University of California, Berkeley, CA 94720, USA.
D. L. Mitchell, Jet Propulsion Laboratory, Mail Stop 300-233, 4800 Oak Grove Drive, Pasadena, CA 91109, USA.
A. L. Sprague, Lunar and Planetary Laboratory, University of Arizona, Tucson, AZ 85721, USA.
I. de Pater, Astronomy Department, University of California, Berkeley, CA 94720, USA.

*To whom correspondence should be addressed.

composition of Mercury at FeO + $TiO_2$ < 6.0% (by weight), corresponding to a lunar rock composition between anorthosite and norite.

The significance of the low iron content of the surface rocks is that partial melting of a chondritic mantle yields liquids enriched in FeO-MgO components (*21*). Current models of Mercury's origin do not justify a mantle composition having an FeO + $TiO_2$ content as low as ~1 to 2% (by weight) (*3, 13*). Thus, we conclude that, within the spatial resolution of the observations, there is no evidence for significant quantities of liquid extracted directly from the mantle having been erupted onto the surface of Mercury after crust formation (*22*). That is, our observations support the theoretically based conclusion that volcanic heat piping has not played a major role in Mercury's thermal evolution.

Laboratory studies of returned lunar samples reveal that the microwave opacities of mare basalts are about two to five times those of highland anorthosites (Fig. 3). In contrast, the lack of residual values in the Caloris Basin (Fig. 1B) indicates that the average microwave opacity in that region must be within 15% of the global average. Overall, currently resolved spatial variations in the FeO + $TiO_2$ abundance are apparently much smaller on Mercury (<5%) than on the moon (>15%).

The preferred composition for Mercury's surface on the basis of microwave data is that of a very Fe- and Ti-depleted rock, possibly anorthosite (by analogy with the lunar crust). This conclusion is in good agreement with observations at visible, near-infrared, and mid-infrared wavelengths (*23, 25*). In particular, a plagioclase-rich crust has been directly inferred from mid-infrared emission spectra of Mercury's surface (*25*). All spectroscopic data thus point to a highly differentiated, lunar highlands–like crust, compatible with the idea that global melting was induced by a late-stage (accretional) giant impact (*11, 12, 25*).

As with the moon, freezing out of a magma ocean has apparently resulted in Mercury becoming a one-plate planet (*3, 5, 26*). Only sluggish convection, and correspondingly ineffective heat transfer, has been possible in the thin mantle remaining after the giant-impact disruption of Mercury (*27*). Thus, with volcanic heat piping having been shut down by cooling and contraction after the impact, as documented by the evidence for compressive tectonics (*26*) as well as by the lack of basaltic volcanism discussed here, the loss of deep internal heat has been limited throughout Mercury's geological evolution. This scenario offers a natural explanation for the apparently contradictory observations of a thin mantle (rapid global cooling) and a planetary magnetic field (molten core).

Our results by no means preclude the occurrence of extensive volcanic units on the surface of Mercury [but see (*1–3*)]. The effect of global contraction, as occurred early in Mercury's geological evolution, is to limit the ability of deep-seated magmas to erupt directly to the surface (*26*). Consequently, one would expect that the upward migration of basaltic liquids generated in the mantle may have been arrested beneath or within the lithosphere, where extensive differentiation can take place (*7*). Secondary eruption of highly differentiated basaltic magma can yield alkaline lavas (*5, 28*); indeed, the presence of alkaline volcanic rocks, including silica-poor (feldspathoid-bearing) eruptives, is in good accord with the mid-infrared spectra of the surface and may offer a natural explanation for the high alkali content of Mercury's atmosphere (*19, 25*). Furthermore, large volumes of impact melt could account for some of Mercury's plains units; recent Clementine spacecraft observations of the moon's south polar region revealed extensive units of shock-melted rock (*29*).

Overall, the observations at microwave, infrared, and visible wavelengths (*15, 23, 25*) provide empirical support for the conclusions of thermal-evolution calculations, which suggest that global magmatic differentiation on Mercury has been limited to crustal and subcrustal intrusion, with minimal extrusive volcanism after formation of the crust (*7*). The lack of volcanic heat piping and the inefficiency of mantle convection have combined to keep the interior of Mercury hot throughout its geological evolution. Our conclusion that extensive basaltic volcanism has not taken place on Mercury's surface is a prediction that can be readily tested by compositional mapping with a space-borne telescope or by future space missions to the innermost planet of the solar system.

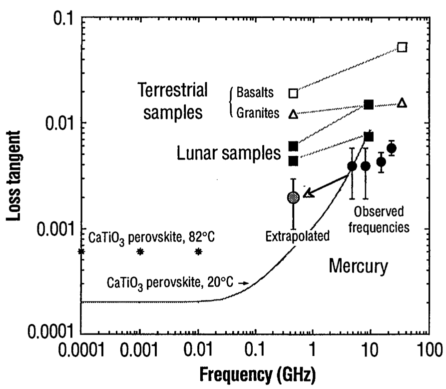


**Fig. 2.** Dielectric loss tangents determined from microwave images of Mercury's surface at 4.8 to 15 GHz (filled circles) are compared with laboratory measurements for samples from the moon (filled squares at 0.45 and 9.4 GHz: upper square, soil 14163; lower square, melt rock 14310) and from Earth (open symbols at 0.45 and 35 GHz: basalts and granites) (*15, 20, 30*). We obtained the Mercury data by assuming (i) no scattering losses and (ii) an effective regolith density of 1.5 g/cm$^3$ in converting from specific loss tangent to the absolute value of loss tangent shown here (*31*). These data are extrapolated to a reference frequency of 0.45 GHz (shaded circle, with error bar reflecting uncertainties both in the observations and in the extrapolation to 450 MHz). Measurements for $CaTiO_3$ perovskite at 20°C (curve) and at 83°C (stars) are from (*17*).

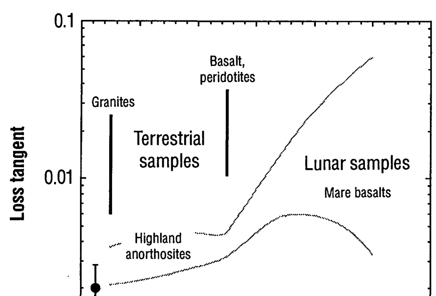


**Fig. 3.** Variation of the 450-MHz dielectric loss tangents of rocks shown as a function of the total FeO + $TiO_2$ content [see (*20*)]. Results for silicic (granites) and mafic or ultramafic (basalts and peridotites) rocks from Earth are summarized (vertical bars) (*30*), along with the field containing all measured values from lunar samples (outlined by shaded curves) (*20*). The solid point indicates the value for Mercury's surface extrapolated to 450 MHz (Fig. 2) and is plotted at the composition derived from the correlation of Heiken *et al.* (*20*) between dielectric loss and bulk composition.

## REFERENCES AND NOTES


1. R. G. Strom, in *The Geology of the Terrestrial Planets*, M. H. Carr, R. S. Saunders, R. G. Strom, D. E. Wilhelms, Eds. (*Publ. NASA SP-469*, National Aeronautics and Space Administration, Washington, DC, 1984), p. 13; R. G. Strom, *Mercury, The Elusive Planet* (Smithsonian Institution, Washington, DC, 1989).
2. F. Vilas, C. R. Chapman, M. S. Matthews, Eds., *Mercury* (Univ. of Arizona Press, Tucson, 1988).
3. S. R. Taylor, *Solar System Evolution* (Cambridge Univ. Press, New York, 1992).
4. N. F. Ness, K. W. Behannon, R. P. Lepping, T. C. Whang, *J. Geophys. Res.* **80**, 2708 (1975); N. F. Ness, *Space Sci. Rev.* **21**, 527 (1978); *Phys. Earth Planet. Inter.* **20**, 209 (1979).
5. Basaltic Volcanism Study Project, *Basaltic Volcanism on the Terrestrial Planets* (Pergamon, New York, 1981).
6. D. J. Stevenson, T. Spohn, G. Schubert, *Icarus* **54**, 466 (1983); G. Schubert, M. N. Ross, D. J. Stevenson, T. Spohn, in (*2*), p. 429.
7. T. Spohn, *Icarus* **90**, 222 (1991).
8. A. E. Ringwood, *Composition and Petrology of the Earth's Mantle* (McGraw-Hill, New York, 1975).
9. H. S. Yoder Jr., *Generation of Basaltic Magma* (National Academy Press, Washington, DC, 1976).
10. Buoyancy, and hence the density of basaltic melt relative to surrounding crystals, appears to limit the maximum depth of basaltic source regions to about 100 km and 500 km for Earth and the moon, respectively [E. Stolper, D. Walker, B. H. Hager, J. F. Hays,

*J. Geophys. Res.* **86**, 6261 (1981)]. Basalts on Mars and Mercury are similarly expected to tap source regions as deep as ~250 km, well below the estimated ~100 to 200 km (past to present) thickness of the lithosphere on Mercury [H. J. Melosh and W. B. McKinnon, in (*2*), p. 374; (*7*)]. Measurements and estimates of mantle plus crust thicknesses range from 2885 km and 2300 to 2950 km for Earth and Venus to 1250 to 1750 km, 1300 to 2100 km, and 500 to 650 km for the moon, Mars, and Mercury, respectively [A. M. Dziewonski and D. L. Anderson, *Phys. Earth Planet. Inter.* **25**, 297 (1981); (*1, 3, 5, 7*)].
11. G. W. Wetherill, in (*2*), p. 670.
12. W. Benz, W. L. Slattery, A. G. W. Cameron, *Icarus* **74**, 516 (1988); A. G. W. Cameron, B. Fegley Jr., W. Benz, W. L. Slattery, in (*2*), p. 692.
13. In particular, we set aside older models that advocate a uniquely refractory-rich composition for Mercury among terrestrial planets [see J. T. Wasson, in (*2*), p. 622; (*3*)].
14. W. B. Tonks and H. J. Melosh, *Icarus* **109**, 326 (1992); J. J. Lissauer and G. R. Stewart, in *Protostars and Planets III*, E. H. Levy and J. I. Lunine, Eds. (Univ. of Arizona Press, Tucson, 1993), p. 1061.
15. D. L. Mitchell and I. de Pater, *Icarus* **110**, 2 (1994).
16. M. J. Ledlow *et al.*, *Astrophys. J.* **384**, 640 (1992).
17. A. R. von Hippel, Ed., *Dielectric Materials and Applications* (MIT Press, Cambridge, MA, 1952). The high dielectric loss is associated with the ferroelectric behavior of the titanate perovskites.
18. J. T. Wasson, in (*2*), p. 622; J. S. Lewis, *ibid.*, p. 651.
19. A. Potter and T. Morgan, *Science* **229**, 651 (1985); *Icarus* **67**, 336 (1986); *Science* **248**, 835 (1990); D. M. Hunten, T. H. Morgan, D. E. Shemansky, in (*2*), p. 562; A. L. Sprague, R. W. H. Kozlowski, D. M. Hunten, *Science* **249**, 1140 (1990); R. M. Killen, A. E. Potter, T. H. Morgan, *ibid.* **252**, 974 (1991).
20. G. H. Heiken, D. T. Vaniman, B. M. French, *Lunar Sourcebook* (Cambridge Univ. Press, New York, 1991).
21. The FeO/MgO molar ratio is enhanced about three- to fivefold in basaltic melt relative to the coexisting peridotitic assemblage of crystals; if we account for the accompanying enrichment in silica, alumina, and other components, the percentage of FeO (by weight) remains constant to within a factor of ~0.5 to 2 between the partial melt and the original source rock [P. L. Roeder and R. F. Emslie, *Contrib. Mineral. Petrol.* **29**, 275 (1970); (*5, 8, 9*)].
22. This conclusion bears on the interpretation of the smooth and intercrater plains of Mercury because their extensive coverage has been a leading argument for their volcanic origin (*1*). Were these plains primarily basaltic, we would have obtained significantly higher values of dielectric loss than were found (*15*).
23. J. Veverka, P. Helfenstein, B. Hapke, J. D. Goguen, in (*2*), p. 37.
24. F. Vilas, *ibid.*, p. 59.
25. A. L. Tyler (Sprague), R. H. W. Kozlowski, L. A. Lebofsky, *Geophys. Res. Lett.* **15**, 808 (1988); A. L. Sprague, R. W. H. Kozlowski, F. C. Witteborn, D. P. Cruikshank, D. H. Wooden, *Icarus* **109**, 156 (1994).
26. S. C. Solomon, *Geophys. Res. Lett.* **5**, 461 (1978); H. J. Melosh and W. B. McKinnon, in (*2*), p. 374.
27. The uniqueness of Mercury in this context is simply due to its proximity to the sun: unlike Earth and Venus, a large fraction of Mercury's mantle excavated during the giant impact falls into the sun rather than reaccumulating, thus explaining the anomalously thin mantle and the resulting sluggish convection (low Rayleigh number) within the planet (*11, 12*). With sublithosphere mantle thicknesses of 400 km, 1100 km, and 2750 km for Mercury, the moon, and Earth (*10*), respectively, scaling arguments yield Rayleigh numbers reduced by ~2.5 and ~1.2 orders of magnitude for Mercury and the moon relative to Earth [R. Jeanloz and S. Morris, *Annu. Rev. Earth Planet. Sci.* **14**, 377 (1986)]. Low Rayleigh numbers, barely higher than the critical value defining the onset of convection, are also found in detailed calculations of Mercury's thermal evolution (*7*).
28. D. W. Hyndman, *Petrology of Igneous and Metamorphic Rocks* (McGraw-Hill, New York, ed. 2, 1982).
29. The Schrödinger Basin area was described by E. M. Shoemaker, M. S. Robinson, and E. M. Eliason [*Science* **266**, 1851 (1994)]. Observations and scaling relations indicate that the volume of shock-induced melt increases rapidly with increasing impact energy and crater size [R. A. F. Grieve and M. J. Cintala, *Meteoritics* **27**, 526 (1992); *ibid.* **28**, 602 (1993)], suggesting that impact-melt units could be more abundant on Mercury's surface than previously recognized [see (*1–3*)].
30. M. J. Campbell and J. Ulrichs, *J. Geophys. Res.* **74**, 5867 (1969).
31. Both of these assumptions are conservative in that scattering losses can only increase the microwave opacity from the value determined by the intrinsic dielectric loss at a given frequency (*15*). Also, a regolith density of 1.5 g/cm³ is in the low range of lunar values (*20*); assuming a higher density for Mercury's regolith would require an even lower dielectric loss tangent to compensate. Thus, our values in Fig. 2 may overestimate the intrinsic dielectric loss tangent of Mercury's surface.
32. We thank I. Carmichael and E. Shoemaker for helpful comments. This work was supported by the National Aeronautics and Space Administration and the National Science Foundation.

4 November 1994; accepted 6 March 1995

# Single Molecule Electron Paramagnetic Resonance Spectroscopy: Hyperfine Splitting Owing to a Single Nucleus

J. Köhler, A. C. J. Brouwer, E. J. J. Groenen, J. Schmidt*

Individual pentacene-$d_{14}$ molecules doped into a *p*-terphenyl-$d_{14}$ host crystal have been studied by optically detected electron paramagnetic resonance spectroscopy. The magnetic resonance transitions between the triplet sublevels of the pentacene molecule and the splitting of the resonance lines for a molecule that contains a carbon-13 nucleus have been observed in an external magnetic field. This splitting is caused by the hyperfine interaction of the triplet electron spin with the single carbon-13 nuclear spin.

In recent years, the feasibility of using spectroscopy in the condensed phase on the level of a single molecule has been demonstrated (*1, 2*). As a result, studies free from the averaging over molecular ensembles that is inherent to conventional spectroscopy became possible, and phenomena such as spectral diffusion (*3–5*), photon bunching (*2, 6*), and antibunching (*7*) have been made visible. Meanwhile, a wealth of experimental techniques have been applied to single molecules in various environments (*8*). In addition, the optical detection of single molecules has been combined with magnetic resonance techniques to make possible the detection of the triplet sublevel transitions of a single pentacene molecule in a *p*-terphenyl host (*9, 10*). The broadening of the triplet transitions owing to the interaction of the single triplet electron spin with a single $^{13}C$ nucleus has been observed through the selective excitation of a pentacene molecule containing a $^{13}C$ nucleus at a particular position (*11*). With this contribution we really enter the domain of magnetic resonance spectroscopy, and we report here the observation of a single triplet electron spin in a external magnetic field.

Thin, sublimation-grown crystals of *p*-terphenyl-$d_{14}$ containing about $10^{-8}$ mol of pentacene-$d_{14}$ per mole of *p*-terphenyl-$d_{14}$ were cooled to 1.2 K. As described in detail in (*11*), the crystals were mounted between a LiF substrate and a quartz cover in the joint focus of a lens and a parabolic mirror. Even for these high-quality crystals, the $S_1 \leftarrow S_0$ transition of pentacene is inhomogeneously broadened owing to the slight differences in the local environments of the guest molecules. Exciting the system by a single-mode laser tuned into the wing of this transition, where the density of absorbers per unit frequency is low, allows the detection of single molecules. The fluorescence emitted to the red of the absorption is collected by the parabolic mirror and recorded by a photomultiplier and photon counting. When the molecule is excited into the $S_1$ singlet state, it can escape from the $S_0 \leftrightarrow S_1$ excitation-emission cycle to the lowest triplet state $T_1$ with a probability of 0.5%. Consequently, the fluorescence photons are emitted in bunches with an average dark period that corresponds to the mean residence time of the molecule in the triplet state. The three sublevels of $T_1$, labeled $T_x$, $T_y$, and $T_z$, are selectively populated and depopulated by intersystem crossing. Because levels $T_x$ and $T_y$ have a short lifetime and a high population probability compared to level $T_z$ (*12*), the mean residence time of a molecule in the triplet state is prolonged under the influence of a microwave field in resonance with the ($T_x$-$T_z$) or ($T_y$-$T_z$) transition. This allows the observation of these magnetic resonance transitions as a decrease in fluorescence [fluorescence-detected magnetic reso-

Center for the Study of Excited States of Molecules, Huygens Laboratory, University of Leiden, Post Office Box 9504, 2300 RA Leiden, Netherlands.

*To whom correspondence should be addressed.